A Theoretical Investigation of the Reaction Between Glycolaldehyde and H^+ and Implications for the Organic Chemistry of Star Forming Regions

Dimitrios Skouteris[1(✉)], Luca Mancini[2], Fanny Vazart[3], Cecilia Ceccarelli[3], Marzio Rosi[4], and Nadia Balucani[2,3]

[1] Master-Up, Via Sicilia 41, 06128 Perugia, Italy
d.skouteris@master-up.it
[2] Dipartimento di Chimica, Biologia e Biotecnologie, Università degli Studi di Perugia, 06123 Perugia, Italy
luca.mancini2@studenti.unipg.it, nadia.balucani@unipg.it
[3] Université Grenoble Alpes, IPAG, 38000 Grenoble, France
{fanny.vazart,cecilia.ceccarelli}@univ-grenoble-alpes.fr
[4] Dipartimento di Ingegneria Civile e Ambientale, Università degli Studi di Perugia, 06125 Perugia, Italy
marzio.rosi@unipg.it

Abstract. The characterization of one of the possible pathways in the reaction between H^+ and glycolaldehyde (the channel leading to COH + CH_3OH^+) has been carried out by performing electronic structure calculations of the stationary points along the minimum energy path. We have employed different theoretical methods verifying that, while geometry optimizations can be performed with a relatively low level of theory, quantitative results for the energies require higher level calculations. The same methodology will be applied to the complete scheme of the title reaction as well as similar processes which are needed to characterize the destruction routes of interstellar complex organic molecules.

Keywords: Computational chemistry methods · Astrochemistry · Electronic structure calculations

1 Introduction

Interstellar medium (ISM) is the non-condensed matter in between stars and their planetary system objects in our Galaxy. It is composed of gas (with the main component being hydrogen) and dust distributed in an inhomogeneous way. On average the number density is extremely low (as low as ~ 0.1 particles per cm^3 in the diffuse warm and ionized regions), but there are regions where baryonic matter becomes denser, the so-called molecular clouds ($\sim 10^4$ particles per cm^3). In some of those regions, new solar systems are formed [1]. The observation of organic molecules of some complexity

© Springer Nature Switzerland AG 2020
O. Gervasi et al. (Eds.): ICCSA 2020, LNCS 12251, pp. 730–743, 2020.
https://doi.org/10.1007/978-3-030-58808-3_53

(hereafter iCOMs for *interstellar complex organic molecules*) in star-forming regions (for a recent survey see [2]) has aroused plenty of interest, since those organic molecules can be the legacy of interstellar chemistry to newly formed planets, thus seeding them with relatively complex organic molecules that behave as the building blocks of life [1, 3–7]. Among the most interesting iCOMS, glycolaldehyde ($HCOCH_2OH$) is the smallest molecule containing both a hydroxyl group and a carbonyl group, thus resembling a sugar. The formation of glycolaldehyde is an intermediate step towards sugars in the formose reaction and, therefore, it is believed to have a strong prebiotic potential. Its detection in high mass and low mass star forming regions [8–12] has posed the question of how a molecule with this degree of complexity can be formed in the harsh conditions of the interstellar medium. Various formation mechanisms have been envisaged involving either gas-phase chemistry or reactions occurring on the icy mantles of interstellar dust grains [13–17]. In particular, the sequence of two neutral-neutral reactions

$$OH + CH_3CH_2OH \rightarrow CH_2CH_2OH + H_2O \quad (1)$$

$$O + CH_2CH_2OH \rightarrow HCOCH_2OH + H \quad (2)$$

seems to be very promising since it is able to reproduce the relative abundance of ethanol (the "mother" molecule) and glycolaldehyde in low mass [13] and high mass [12] star forming regions.

In both cases, whether released in the gas phase from the sublimating icy mantles of the interstellar dust grains or formed directly in the gas phase, to build up realistic astrochemical models and account for the observed abundances it is necessary to characterize the destruction routes of each species in the gas phase. Unfortunately, there are no data available in the literature concerning the possible destruction routes of glycolaldehyde. In the conditions of the ISM, most molecules are consumed by their reactions with energetic ions, such as HCO^+, H_3^+, He^+ and H^+ (see for instance [18]), which are abundant in the ISM. While in the case of the reactions with the ions HCO^+ and H_3^+ the most probable outcome is a proton transfer mechanism and in the case of He^+ only a charge transfer mechanism is possible, the collisions of interstellar molecules with H^+ can occur either by charge transfer (in this case the molecule is ionized and can also undergo dissociative ionization) or by a real chemical reaction, in which H^+ adds to the molecule and a reaction pathway starts.

Given the paucity of information on the processes following the interaction of iCOMs with H^+, in our laboratory we have decided to start a systematic investigation of these processes by resorting to electronic structure calculations of the stationary points along the relevant potential energy surfaces (PESs) and kinetics estimates. In this contribution, we present the first results concerning the reactive pathway

$$HCOCH_2OH + H^+ \rightarrow COH + CH_3OH^+ \quad (3)$$

Different theoretical methods have been tested and compared to assess their performance and select the best method for our planned systematic investigation of iCOMs reactions.

2 Computational Details

The characterization of the PES for the reaction (3) has been performed by locating the lowest stationary points with different computational strategies listed in Table 1.

Table 1. List of combinations method/basis set used.

Method	Basis set
MP2	6-31G(d,p)
B3LYP	STO-3G
B3LYP	aug-cc-pVDZ
B3LYPD3	aug-cc-pVDZ
B2PLYP	aug-cc-pVTZ
B2PLYPD3	aug-cc-pVTZ

Glycolaldehyde is characterized by four possible conformers, among which the *cis-cis* structure is the most stable one because of an intramolecular hydrogen bond. Therefore, we have performed our calculations starting from the *cis-cis* conformer (see Fig. 2). As an example, the structures of this conformer of glycolaldehyde as obtained with the different methods are reported in Fig. 1. A few other stationary points have been also characterized using the methods listed in Table 1.

Subsequently, the geometries of all the stationary points, including reactants and products, have been optimized only at the B3LYP level of theory [19, 20], in conjunction with the correlation consistent aug-cc-pVTZ basis set [21–23]. Harmonic vibrational frequencies have been computed at the same level of theory, in order to define the nature of the identified stationary points, *i.e.,* minimum if all the frequencies are real, saddle point if there is one and only one imaginary frequency. The identified saddle point has been assigned through Intrinsic Reaction Coordinates (IRC) calculations [24, 25]. The zero-point-energy correction (computed using the scaled harmonic vibrational frequencies) has been added in order to correct the energies at 0 K. All calculations have been repeated (to assess the accuracy of the obtained data) with the double hybrid B2PLYP functional in addition to the contribution of the semiempirical dispersion considered in the D3BJ model (B2PLYPD3) [26, 27], with the same aug-cc-pVTZ basis set. In the end, coupled-cluster single and double excitations augmented by a perturbative treatment of the triple excitations (CCSD(T)) [28–30] calculations have been performed with the same basis set and the B2PLYPD3/aug-cc-pVTZ optimized geometries, following a computational scheme which has been used in previous cases [31–38]. In addition, computational work has been carried out in order to establish which combination of method and basis set would be the most suitable one for the analyzed reaction. All calculations have been performed using Gaussian 09 [39] while the analysis of the vibrational frequencies has been done using Avogadro [40, 41].

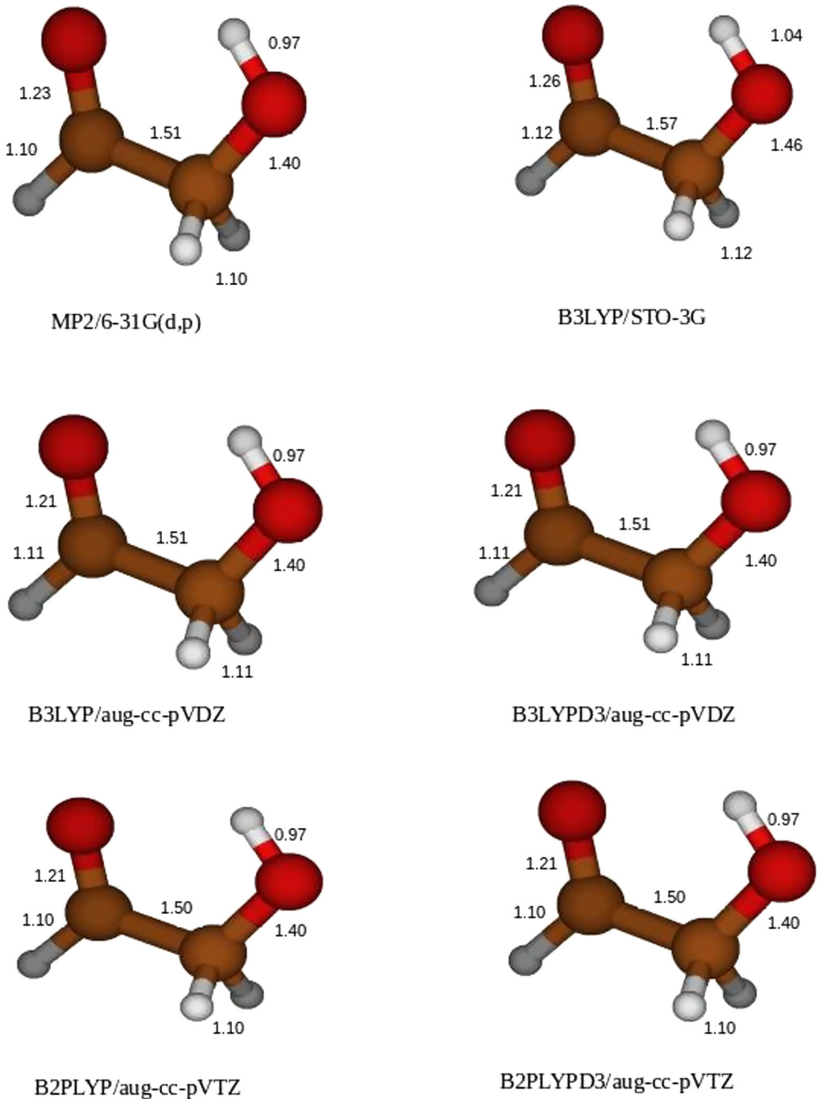

Fig. 1. Principal bond lengths (in Å) of the molecule glycolaldehyde calculated at different levels of theory.

3 Results and Discussion

The complete potential energy surface obtained for the reaction (3) is reported in Fig. 2, with the geometries optimized at the B3LYP/aug-cc-pVTZ level of theory. In particular, in the figure the energies have been reported at the B3LYP/aug-cc-pVTZ (in red), B2PLYPD3/aug-cc-pVTZ (in black) and CCSD(T)/aug-cc-pVTZ (in black, in

parentheses) levels of theory. In order to have an analysis of the minimum energy path, the more accurate CCSD(T) energies are considered.

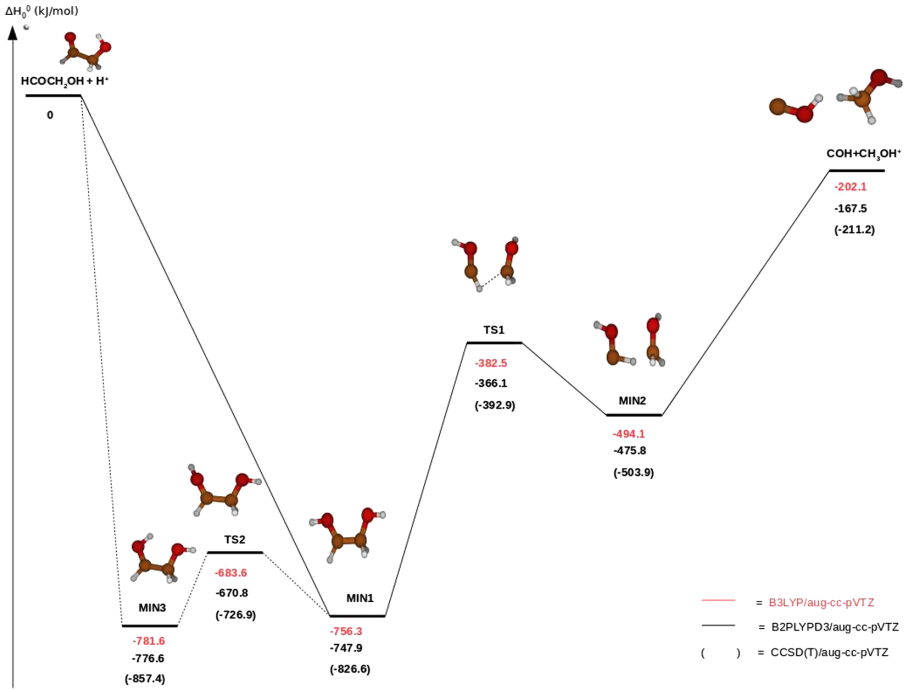

Fig. 2. Potential energy surface obtained, with the geometries optimized at the B3LYP/aug-cc-pVTZ level of theory. The energies have been reported at the B3LYP/aug-cc-pVTZ (in red), B2PLYPD3/aug-cc-pVTZ (in black) and CCSD(T)/aug-cc-pVTZ (in black, in parentheses) levels of theory. (Color figure online)

There are two possible attack sites for the incoming free proton.

In the initial approach analyzed in this work, the reaction starts with a barrierless addition of the proton to the oxygen of the carbonyl group of the molecule, leading to the formation of MIN1, in which a new O-H bond is formed at a distance of 0.977 Å, while the value of the C-O bond length goes from 1.206 Å to 1.261 Å, indicating a double-to-single bond variation. The energy of the stationary point, with respect to the reactant energy asymptote, taken as a reference, is −826.6 kJ/mol. The alternative additional initial approach can feature, instead, the addition of H^+ on the oxygen of the hydroxyl group (the investigation of this pathway is currently under way).

Starting from MIN1, it is possible to obtain the second minimum in the PES, named MIN2. In this case the C-C bond is broken and two fragments are formed: HCOH and CH_2OH. In this structure, the hydrogen atom linked to the carbon in the HCOH fragment strongly interacts with the carbon atom in the CH_2OH fragment at a distance of 1.351 Å and the total charge is distributed over the complex. The relative energy of MIN2, with respect to the reactant energy asymptote, is −503.9 kJ/mol. The transition from MIN1 to MIN2 is possible through the overcoming of a barrier of 433.7 kJ/mol. The related transition state, TS1, clearly shows the breaking of the C-C bond. The distance between the two C atoms, indeed, is increased up to 2.146 Å. The analysis of the vibrational frequencies for TS1 allows us to notice the interaction of the H in the HCOH fragment with the carbon atom in the CH_2OH moiety. The distance between the two mentioned atoms is 1.924 Å. Once formed, MIN2 directly leads to the formation of the two products (HCO and CH_3OH^+), located at 211.2 kJ/mol below the reactant energy asymptote. No transition states have been found for this process. In general, it is possible to notice that all the identified stationary points lie below the reactant energy asymptote, so the reaction is globally exothermic and can take place in the harsh conditions of the interstellar medium.

The analysis of the stationary points in the PES has been performed at different levels of theory; in Figs. 3, 4 are reported the values of the bond lengths (in Å) resulting from the geometry optimized at B3LYP/aug-cc-pVTZ (in red) and B2PLYPD3/aug-cc-pVTZ (in black) level of theory. As can be seen from the reported data, there are no particular differences in the bond lengths evaluated with the two different computational strategies. The only appreciable difference is shown in the C-H interaction in TS1, in which the chemical bond is not completely formed. In this case the B2PLYPD3/aug-cc-pVTZ combination provides a length which is 0.031 Å lower than the one resulting from the B3LYP/aug-cc-pVTZ calculation. A different behavior can be seen from the analysis of the energies. In Tables 2, 3, 4 are reported the enthalpy changes and barrier heights at 0 K, computed at the three previously mentioned levels of theory.

Since the geometries of the different stationary points are very similar, it is possible to conclude that the differences in energies are related to the differences in the two methods. In particular the B2PLYPD3 functional, in addition to the D3BJ dispersion, includes a contribution related to second order perturbation theory, which can be considered the origin of the noticed differences. The same conclusion can be reached considering the results coming from the use of different methods and basis sets. As can be seen in the results shown in Fig. 1, in the case of glycolaldehyde there are no particular differences in the values of the bond lengths evaluated at different levels of theory. The results are, instead, more varied for the MIN2 and TS1 structures. The main differences can be noticed when the B3LYP functional is used in conjunction with the

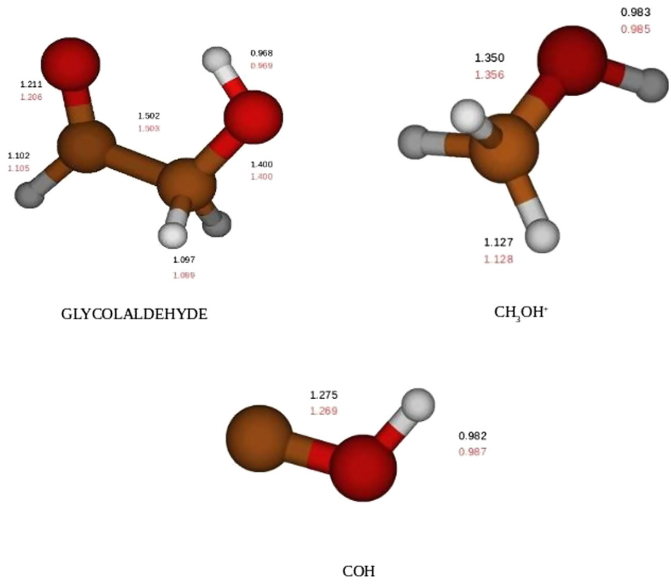

Fig. 3. Values of the bond lengths (in Å) resulting from the geometry optimized at B3LYP/aug-cc-pVTZ (in red) and B2PLYPD3/aug-cc-pVTZ (in black) levels of theory for the reactant and products of the reaction. (Color figure online)

STO-3G basis set. From a comparison with the cases in which the same functional is used together with other different basis sets, it can be concluded that the differences in the bond lengths derive mainly from the use of the STO-3G basis set, which is less accurate since it is a minimum basis set. From an energetic point of view, it can be noticed that the combination that most differs from the reference (which in this case is the CCSD(T) energy calculation) is once again due to the use of the STO-3G basis set. The values of the energy obtained at different levels of theory are shown in Table 5. In some cases, the results obtained at the B3LYP level of theory seem to be closer to the CCSD(T) values (which is considered the best approach) than the ones obtained at the B2PLYPD3 level. However, the B2PLYPD3/aug-cc-pVTZ approach tends to give a more accurate estimate for the barrier heights, a crucial aspect when it comes to deriving rate coefficients and product branching ratios (Figs. 5 and 6).

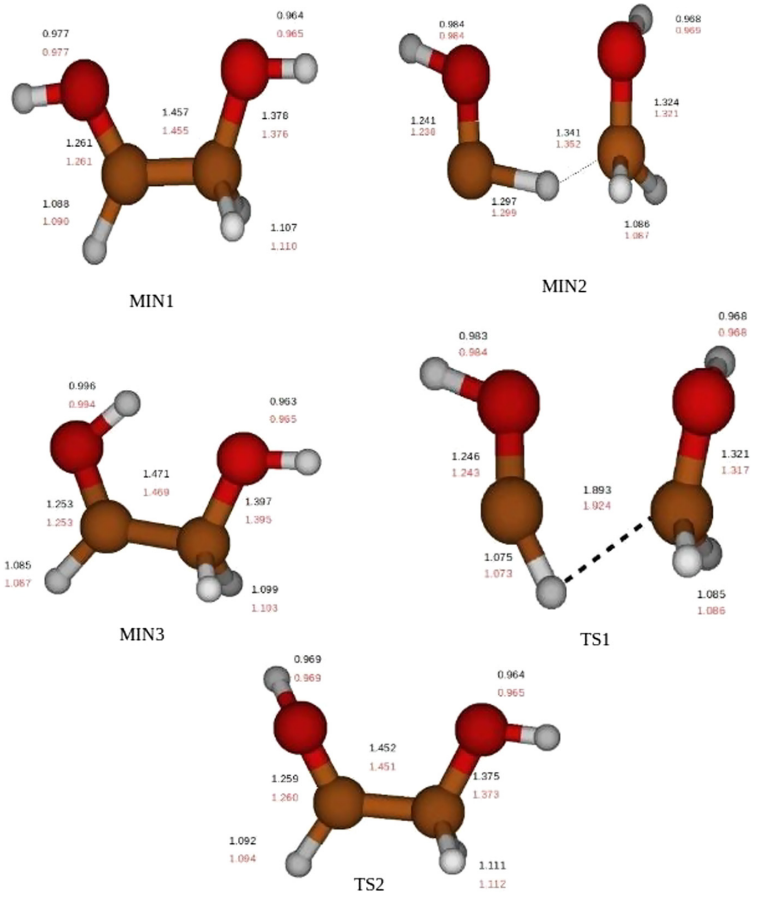

Fig. 4. Values of the bond lengths (in Å) resulting from the geometry optimized at B3LYP/aug-cc-pVTZ (in red) and B2PLYPD3/aug-cc-pVTZ (in black) levels of theory for the identified minima and transition states. (Color figure online)

Table 2. Enthalpy changes and barrier heights (in kJ/mol) for the system, evaluated at the B3LYP/aug-cc-pVTZ level of theory.

	$\Delta H°_0$	Barrier heights
$H^+ + HCOCH_2OH \rightarrow$ MIN1	−756.3	
MIN1 → MIN2	262.2	373.8
MIN1 → MIN3	−25.3	72.7
MIN2 → $COH + CH_3OH^+$	292.0	

Table 3. Enthalpy changes and barrier heights (in kJ/mol) for the system, evaluated at the B2PLYPD3/aug-cc-pVT level of theory.

	$\Delta H°_0$	Barrier heights
$H^+ + HCOCH_2OH \rightarrow MIN1$	−747.9	
$MIN1 \rightarrow MIN2$	272.1	381.8
$MIN1 \rightarrow MIN3$	−28.7	77.1
$MIN2 \rightarrow COH + CH_3OH^+$	308.3	

Table 4. Enthalpy changes and barrier heights (in kJ/mol) for the system, evaluated at the CCSD(T)/aug-cc-pVTZ level of theory considering the geometry optimized at the B2PLYPD3/aug-cc-pVTZ level of theory.

	$\Delta H°_0$	Barrier heights
$H^+ + HCOCH_2OH \rightarrow MIN1$	−826.6	
$MIN1 \rightarrow MIN2$	322.7	433.7
$MIN1 \rightarrow MIN3$	−30.8	99.7
$MIN2 \rightarrow COH + CH_3OH^+$	292.7	

Table 5. Energy values (in kJ/mol) of the different stationary points with respect to the reactant energy asymptote at different levels of theory

Level of theory	TS1	MIN2
MP2/6-31G(d,p)	−339.2	−462.1
B3LYP/STO-3G	−538.0	−680.8
B3LYP/aug-cc-pVDZ	−376.9	−490.8
B3LYPD3/aug-cc-pVDZ	−379.6	−492.1
B2PLYP/aug-cc-pVTZ	−365.0	−475.3
B2PLYPD3/aug-cc-pVTZ	−366.1	−476.0

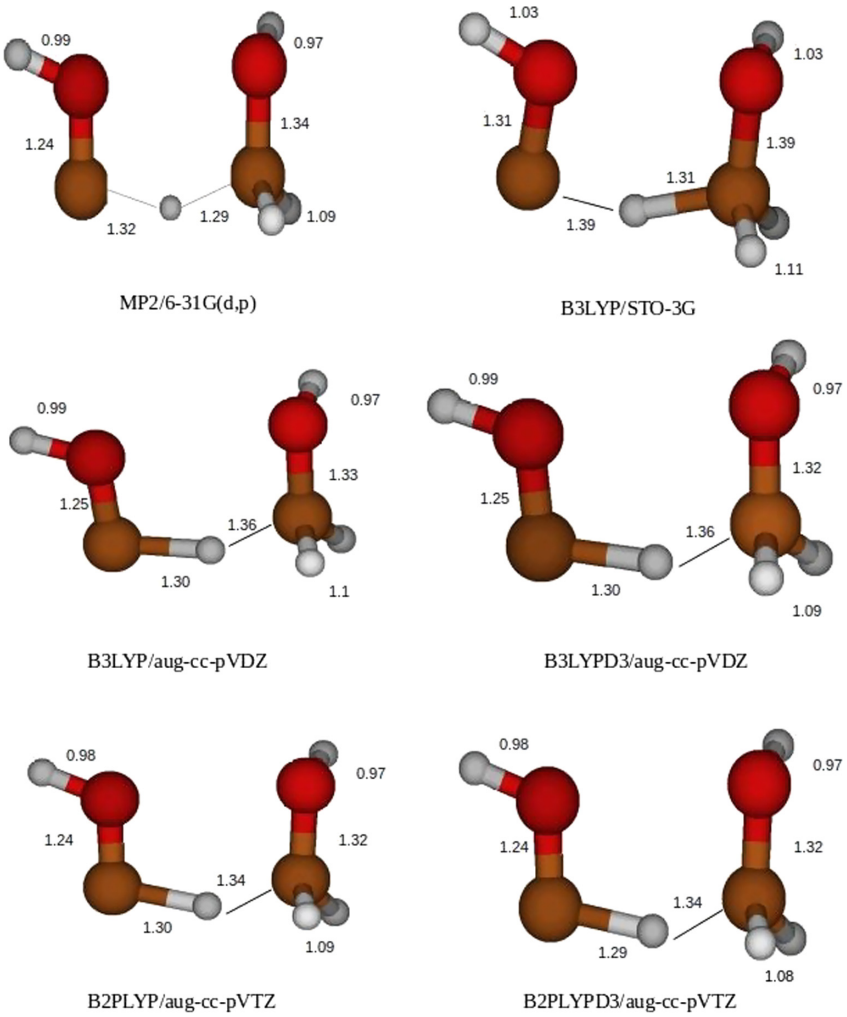

Fig. 5. Principal bond lengths (in Å) of the minimum MIN2 calculated at different levels of theory

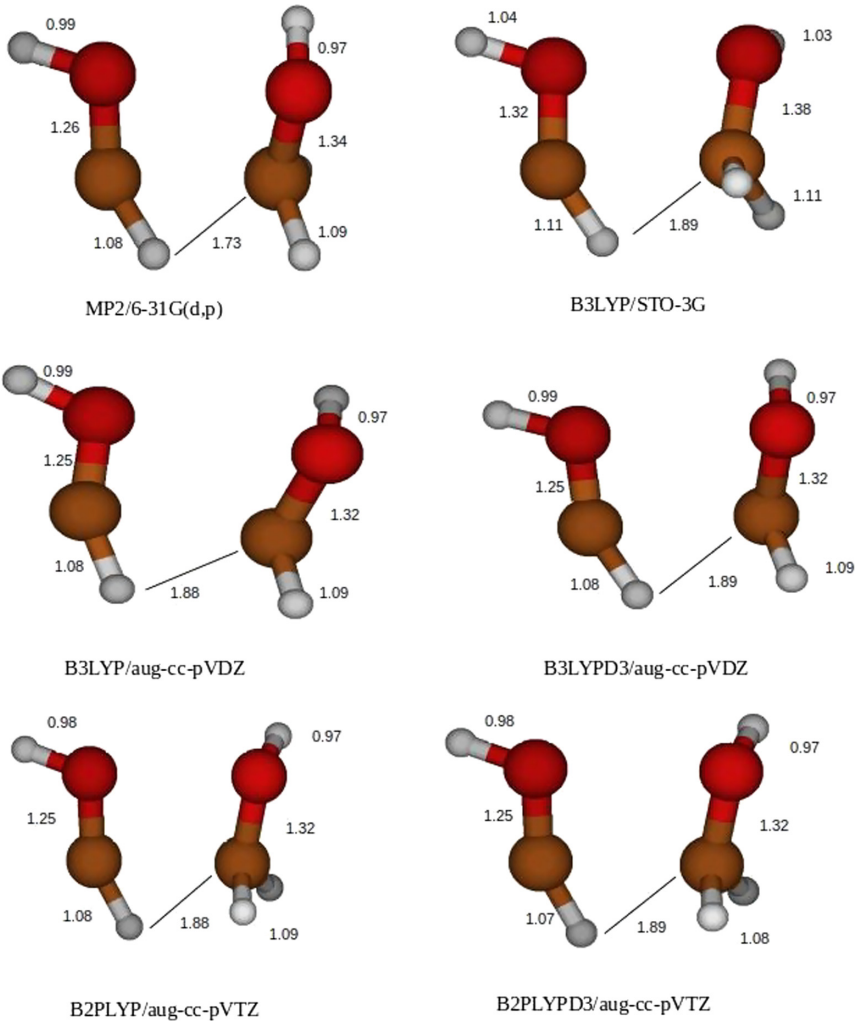

Fig. 6. Principal bond lengths (in Å) of the transition state TS1 calculated at different levels of theory.

4 Conclusion

In this work, different ab initio methods have been employed for the study of the reaction between H^+ and glycolaldehyde with the addition site on the oxygen of the carbonyl group and with the formation of COH and CH_3OH^+. The aim was to define the best compromise between chemical accuracy and computational costs. The best approach will be later employed in our systematic investigation of this and similar reactions. From the data analyzed we can conclude that relatively low-level calculations, such as B3LYP/aug-cc-pVTZ, can be used for geometry optimization and harmonic vibrational frequencies calculations. However, the energy must be evaluated at a higher level of theory, *e.g.* CCSD(T), in order to obtain more accurate values and construct a realistic potential energy surface. This conclusion is in agreement with previous work.

The reaction channel investigated in this contribution is only part of the PES of the glycolaldehyde-H^+ system. The global PES is expected to be much more complex with other possible exit channels (namely, those leading to the products $HCOH^+ + H_2COH$, $HCOH + H_2COH^+$, $H_2 + HCOHCHO^+$, $H_2O + CH_2COH^+$, $H_2 + OCCH_2OH^+$, $H_3O^+ + OCCH_2$ and $H_2O + CH_3CO^+$). Another complication is due to the presence of a second site for H^+ addition. Having verified that a combined B3LYP/aug-cc-pVTZ and CCSD(T) approach is a viable method to characterize the PES of this system, further investigations complemented by kinetics calculations are needed. We aim to complete those calculations to provide reliable estimates of the rate coefficients to be employed in astrochemical models.

Acknowledgments. This project has received funding from the European Research Council (ERC) under the European Union's Horizon 2020 research and innovation programme, for the Project "The Dawn of Organic Chemistry" (DOC), grant agreement No 741002 and from the European Union's Horizon 2020 research and innovation programme under the Marie Sklodowska-Curie grant agreement No 811312 for the project "Astro-Chemical Origins" (ACO). M.R. acknowledges the project "Indagini teoriche e sperimentali sulla reattività di sistemi di interesse astrochimico" funded by Fondo Ricerca di Base 2018 of the University of Perugia. DS wishes to thank "Master-Up" for funding.

References

1. Caselli, P., Ceccarelli, C.: Our astrochemical heritage. Astron. Astrophys. Rev. **20**, 56 (2012)
2. McGuire, B.A.: 2018 Census of interstellar, circumstellar, extragalactic, protoplanetary disk, and exoplanetary molecules. Astrophys. J. Suppl. Ser. **239**, 2 (2018)
3. Ceccarelli, C., et al.: Seeds Of Life In Space (SOLIS): The Organic Composition Diversity at 300–1000 au Scale in Solar-type Star-forming Regions. ApJ, 850 (2017)
4. Herbst, E., van Dishoeck, E.F.: Complex organic interstellar molecules. Annu. Rev. Astron. Astrophys. **47**(1), 427–480 (2009)
5. Balucani, N.: Elementary reactions and their role in gas-phase prebiotic chemistry. Int. J. Mol. Sci. **10**, 2304–2335 (2009)

6. Balucani, N.: Elementary reactions of N atoms with hydrocarbons: first steps towards the formation of prebiotic N-containing molecules in planetary atmospheres. Chem. Soc. Rev. **41**, 5473–5483 (2012)
7. Ehrenfreund, P., Charnley, S.B.: Organic molecules in the interstellar medium, comets, and meteorites: a voyage from dark clouds to the early earth. Ann. Rev. Astron. Astrophys. **38**, 427–483 (2000)
8. Hollis, J.M., Lovas, F.J., Jewell, P.R. Interstellar Glycolaldehyde: The First Sugar. ApJ, 540, 2, L107–L110 (2000)
9. Lefloch, B., et al.: L1157-B1, a factory of complex organic molecules in a solar-type star-forming region. MNRAS **469**, L73 (2017)
10. Jørgensen, J.K., et al.: The ALMA Protostellar Interferometric Line Survey (PILS). First results from an unbiased submillimeter wavelength line survey of the Class 0 protostellar binary IRAS 16293–2422 with ALMA. Astron. Astrophys. 595, A117 (2016)
11. Bouchez, A., et al.: The submillimeter spectrum of deuterated glycolaldehydes. Astron. Astrophys. **540**, A51 (2012)
12. Xue, C., Remijan, A.J., Burkhardt, A.M., Herbst, E.: ALMA observations of the spatial distribution of three $C_2H_4O_2$ isomers toward Sgr B_2(N). ApJ **871**, 1 (2019)
13. Skouteris, D., et al.: The genealogical tree of ethanol: gas-phase formation of glycolaldehyde, acetic acid, and formic acid. ApJ **854**, 2 (2018)
14. Coutens, A., et al.: Chemical modelling of glycolaldehyde and ethylene glycol in star-forming regions. MNRAS **475**(2), 2016–2026 (2018)
15. Chuang, K.-J., Fedoseev, G., Ioppolo, S., van Dishoeck, E.F., Linnartz, H.: H-atom addition and abstraction reactions in mixed CO, H_2CO and CH_3OH ices - an extended view on complex organic molecule formation. MNRAS **455**(2), 1702–1712 (2016)
16. Garrod, R.T., Widicus, S.L.V., Herbst, E.: Complex chemistry in star-forming regions: an expanded gas-grain warm-up chemical model. ApJ **682**(1), 283–302 (2008)
17. Holdship, J., Rawlings, J., Viti, S., Balucani, N., Skouteris, D., Williams, D.: Investigating the efficiency of explosion chemistry as a source of complex organic molecules in TMC-1. ApJ **878**, 65 (2019)
18. Ascenzi, D., et al.: Destruction of dimethyl ether and methyl formate by collisions with He^+. Astron. Astrophys. **625**, A72 (2019)
19. Becke, A.D.: A new mixing of Hartree-Fock and local density functional theories. J. Chem. Phys. **98**(2), 1372–1377 (1998)
20. Stephens, P.J., Devlin, F.J., Chablowski, C.F., Frisch, M.J.: Ab initio calculation of vibrational absorption and circular dichroism spectra using density functional force fields. J. Phys. Chem. **98**(45), 11623–11627 (1994)
21. Dunning Jr., T.H.: Gaussian basis sets for use in correlated molecular calculations. I. The atoms boron through neon and hydrogen. J. Chem. Phys. **90**, 1007–1023 (1989)
22. Woon, D.E., Dunning Jr., T.H.: Gaussian basis sets for use in correlated molecular calculations. III. The atoms aluminum through argon. J. Chem. Phys. **98**, 1358–1371 (1993)
23. Kendall, R.A., Dunning Jr., T.H., Harrison, J.R.: Electron affinities of the first row atoms revisited. Systematic basis sets and wave functions. J. Chem. Phys. **96**, 6796–6806 (1992)
24. Gonzalez, C., Schlegel, H.B.: An improved algorithm for reaction path following. J. Chem. Phys. **90**, 2154–2161 (1989)
25. Gonzalez, C., Schlegel, H.B.: Reaction path following in mass-weighted internal coordinates. J. Phys. Chem. **94**, 5523–5527 (1990)
26. Goerigk, L., Grimme, S.: Efficient and accurate double-hybrid-meta-GGA density functionals- evaluation with the extended GMTKN30 database for general main group thermochemistry, kinetics and noncovalent interactions. J. Chem. Theory Comput. **7**, 291–309 (2011)

27. Grimme, S., Ehrlich, S., Goerigk, L.: Effect of the damping function in dispersion corrected density functional theory. J. Comput. Chem. **32**, 1456–1465 (2011)
28. Bartlett, R.J.: Many-body perturbation theory and coupled cluster theory for electron correlation in molecules. Ann. Rev. Phys. Chem. **32**, 359–401 (1981)
29. Raghavachari, K., Trucks, G.W., Pople, J.A., Head-Gordon, M.: Quadratic configuration interaction. A general technique for determining electron correlation energies. Chem. Phys. Lett. **157**, 479–483 (1989)
30. Olsen, J., Jorgensen, P., Koch, H., Balkova, A., Bartlett, R.J.: Full configuration–interaction and state of the art correlation calculations on water in a valence double-zeta basis with polarization functions. J. Chem. Phys. **104**, 8007–8015 (1996)
31. Vazart, F., Calderini, D., Puzzarini, C., Skouteris, D., Barone, V.: State-of-the-art thermochemical and kinetic computations for astrochemical complex organic molecules: formamide formation in cold interstellar clouds as a case study. J. Chem. Theory Comput. **12**, 5385–5397 (2016)
32. Falcinelli, S., Rosi, M., Cavalli, S., Pirani, F., Vecchiocattivi, F.: Stereoselectivity in autoionization reactions of hydrogenated molecules by metastable noble gas atoms: the role of electronic couplings. Chem. Eur. Jour. **22**(35), 12518–12526 (2016)
33. Leonori, F., et al.: Crossed-beam and theoretical studies of the $S(^1D) + C_2H_2$ reaction. J. Phys. Chem. A **113**(16), 4330–4339 (2009)
34. Bartolomei, M., et al.: The intermolecular potential in NO-N2 and (NO-N2) + systems: implications for the neutralization of ionic molecular aggregates. PCCP **10**(39), 5993–6001 (2008)
35. de Petris, G., Cartoni, A., Rosi, M., Barone, V., Puzzarini, C., Troiani, A.: The proton affinity and gas-phase basicity of sulfur dioxide. ChemPhysChem **12**(1), 112–115 (2011)
36. Leonori, F., et al.: Observation of organosulfur products (thiovinoxy, thioketene and thioformyl) in crossed-beam experiments and low temperature rate coefficients for the reaction $S(^1D) + C_2H_4$. Phys. Chem. Chem. Phys. **11**(23), 4701–4706 (2009)
37. de Petris, G., Rosi, M., Troiani, A.: SSOH and HSSO radicals: an experimental and theoretical study of [S2OH]0/± species. J. Phys. Chem. A **111**(28), 6526–6533 (2007)
38. Rosi, M., Falcinelli, S., Balucani, N., Casavecchia, P., Leonori, F., Skouteris, D.: Theoretical study of reactions relevant for atmospheric models of titan: interaction of excited nitrogen atoms with small hydrocarbons. In: Murgante, B., Gervasi, O., Misra, S., Nedjah, N., Rocha, A.M.A.C., Taniar, D., Apduhan, B.O. (eds.) ICCSA 2012. LNCS, vol. 7333, pp. 331–344. Springer, Heidelberg (2012). https://doi.org/10.1007/978-3-642-31125-3_26
39. Gaussian 09, Revision A.02, Frisch, M.J., et al.: Gaussian, Inc., Wallingford CT (2009)
40. Avogadro: an open-source molecular builder and visualization tool. Version 1.XX. (http://avogadro.cc)
41. Hanwell, M.D., Curtis, D.E., Lonie, D.C., Vandermeersch, T., Zurek, E., Hutchison, R.: Avogadro: an advanced semantic chemical editor, visualization, and analysis platform. J. Cheminformatics **4**, 17 (2012)